# An investigation of the migration of oxygen deficiencies in the superconductor $YBa_2Cu_3O_{7\delta}$



1989 J. Phys.: Condens. Matter 1 6939

(http://iopscience.iop.org/0953-8984/1/39/004)

J. Phys.: Condens. Matter 1 (1989) 6939–6950. Printed in the UK

# An investigation of the migration of oxygen deficiencies in the superconductor $YBa_2Cu_3O_{7-\delta}$

J X Zhang†, G M Lin†, Z C Lin†, K F Liang†, P C W Fung‡ and G G Siu§

† Department of Physics, Zhongshan University, Guangzhou, People's Republic of China
‡ Physics Department, University of Hong Kong, Hong Kong
§ Department of Applied Science, City Polytechnic of Hong Kong, Hong Kong

Received 21 September 1988, in final form 6 February 1989

**Abstract.** The temperature and oscillation frequency dependences of internal friction and shear modulus of superconducting $YBa_2Cu_3O_{7-\delta}$ specimens are measured using a multi-function internal-friction torsion pendulum to study the degree of ordering and the migration of oxygen deficiency sites in the superconductor $YBa_2Cu_3O_{7-\delta}$. It is found that relaxation is most likely to occur in units where one oxygen site is surrounded by four barium ions rather than along the O–Cu–O chain. This indicates that an internal-friction study provides a powerful way of investigating the relaxation process of oxygen atoms as well as the degree of ordering of oxygen deficiencies in relation to superconductivity features.

## 1. Introduction

In cuprate superconductors, not only is copper a crucial element, but also oxygen deficiencies play a crucial role in their superconductivity. The effect of oxygen stoichiometry on crystal structure, namely the orthorhombic-to-tetragonal phase transition (Jorgensen *et al* 1987, David *et al* 1987, Miceli *et al* 1988), and on the charge-transport properties (Van Tendeloo *et al* 1987) has been studied extensively. The oxygen concentration is speculated to be the cause of the observed symmetry transformation (Derouane *et al* 1987) and it is expected that oxygen vacant sites will be ordered as the crystal becomes a superconductor. The activation energy of the oxygen ion motion has been estimated (Strobel *et al* 1987). An internal-friction (IF) study of the dynamics of oxygen vacancies has been carried out; preliminary results of possible oxygen ion migration between oxygen sites are reported, and the corresponding activation energy is obtained (Chen *et al* 1987).

In this paper, we use the low-frequency IF probe to investigate the relaxation process in a Y–Ba–Cu–O specimen. We present results of *in situ* IF measurements as a function of temperature. Such a study confirms the existence of one relaxation process of ordered or disordered oxygen vacant sites and a second relaxation process of ordered oxygen vacant sites. These processes are related to the superconducting properties before IF measurements. They may provide clues to elucidating the relative importance of the $CuO_2$ planes and Cu–O chains, and a better understanding of dynamic processes in cuprate superconductors.

0953-8984/89/396939 + 12 $02.50  

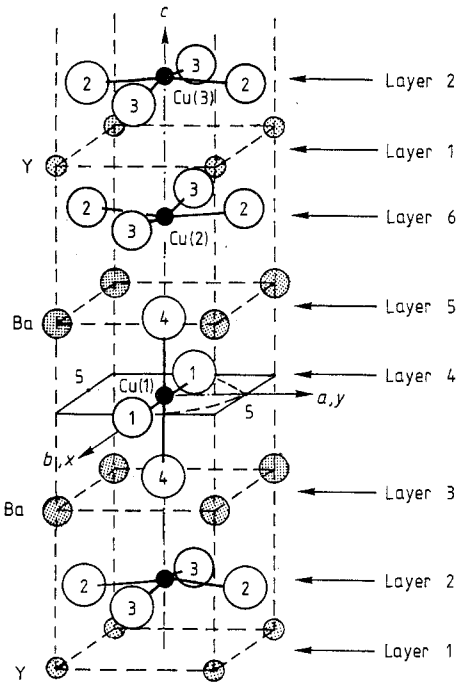


**Figure 1.** Schematic representation of the crystal structure of $YBa_2Cu_3O_{7-\delta}$

A unit cell of the $YBa_2Cu_3O_7$ crystal (figure 1) has six layers which are almost parallel to each other. All layers except layer 1 have oxygen ions which may move away, leaving vacant sites. The following questions are important to the understanding of these crystals.

(i) At which layers are oxygen vacancies most likely to be generated?
(ii) Between which layers will oxygen vacancy migration dominate?
(iii) What is the time sequence of the relaxation processes?
(iv) What are the values of the corresponding activation energies?

An IF study is suitable for investigating these relaxation processes. If $\omega$ is the oscillation frequency, IF peaks appear at $\omega\tau = 1$, where $\tau$ is the relaxation time. Once the peak is allocated for a frequency $\omega$, $\tau$ and therefore the activation energy $H$ can be determined (as $\tau_p = \tau_0 \exp(H/k\tau_p)$, where p pertains to a peak and $k$ is the Boltzmann constant). The relaxation strength $\Delta$ is obtained directly from the peak height. According to the point-defect relaxation theory, if interactions exist between point defects or within a special configuration of point defects, the temperature dependence of $\Delta$ will be analogous to the Curie–Weiss law:

$$\Delta \propto (T - T_c')^{-1}$$

where $T_c'$ is the critical temperature for a 'self-induced' ordering. The interaction energy $E_i$ can thus be obtained from $T_c'$: $E_i = kT_c'$.

The ordering concept in this paper is adopted in a general sense, e.g. a chemical decomposition is interpreted as a change from order to disorder.

## 2. Sample preparation and experiment

$Y_2O_3$ (purity, 99.99%), CuO (analytical reagent grade) and $BaCO_3$ (commercial purity grade) in a predetermined ratio are dissolved in acetic acid with a small amount of nitric acid. The standard co-precipitation method was used to obtain Y–Ba–Cu–O powder (Luo *et al* 1987). The powder was compressed into a rectangular piece of approximate size 1 mm × 4 mm × 60 mm and sintered on a MgO plate at 945 °C for 6 h. A second 6 h sintering was carried out after turning the sintered piece upside down and then it was cooled to room temperature in the oven. Oxygen atmosphere treatment of the piece lasted for 1 h at 650 °C and cooling to room temperature took another 3 h. The procedure for preparing the Y–Ba–Cu–O sample is essentially identical with previous reports (Luo *et al* 1987, Lin *et al* 1988) except that second sintering process was used to obtain a thorough solid state reaction of the whole bulk.

The experiment comprises four thermal cycles, each of which includes a heating process from room temperature to 623 K, a period of constant temperature (623 K) and cooling to room temperature, as shown in table 1.

**Table 1.** Conditions for the samples (the figures referred to are given in § 3).

| 77 K | Room temperature; 1 atm pressure | Pressure, 60 Torr; temperature rise in steps of 5 K | 623 K |
|---|---|---|---|
| Figure 3(*b*) ← | (i) | → Figure 3(*a*) (first thermal cycle) | ≈ 15 min |
| Figure 4(*b*) ← | (ii) | → Figure 4(*a*) (second thermal cycle) | ≈ 15 min |
| | (iii) | → Figure 5 (third thermal cycle) | Evacuated for 2 h ($10^{-2}$ Torr) |
| Figure 6(*b*) ← | (iv) | → Figure 6(*a*) (fourth thermal cycle) | |

The experiment is carried out at a low pressure of 60 Torr for the first and second cycles, and for the heating stage of the third cycle the pressure is lowered to $10^{-2}$ Torr during the subsequent 623 K constant-temperature stage and maintained until the end of the last cycle. The constant-temperature period lasts for 15 min in the first and second cycles. Heating at a low pressure, in general, benefits oxygen desorption but oxygen desorption happens mainly during the constant-temperature stage because the oxygen ions are most mobile when the temperature is highest and for the long 'retaining time'. In the third cycle the constant-temperature period is prolonged to 2 h to obtain more oxygen desorption. At the beginning of each thermal cycle, specimen characterisation is performed. Then the IF $Q^{-1}$ and the relative shear modulus $G$ are measured at five selected frequencies in the range $10^{-2}$–10 Hz with forced oscillation and a strain amplitude of $5 \times 10^{-6}$ during the increasing-temperature process. The oxygen stoichiometry is expected to decrease monotonically with increase in cycle number.

Four pieces of 1 mm × 1 mm × 10 mm ceramic pellets are cut from the sample as references. These were characterised using x-ray diffraction for structure identification and four-terminal resistivity measurements were used to check the electrical behaviour; the mutual inductance method was also employed for AC susceptibility measurements. There is no distinct difference between the characterisation results of the first piece (before thermal cycling starts) and those reported in previous work (Luo *et al* 1987, Lin *et al* 1988); an inductively coupled plasma emission spectrometer was used to examine the sample composition, which is Y : Ba : Cu = 1 : (2 ± 0.05) : (3 ± 0.05). Figure 2 shows $R$–$T$ curves for the first reference piece ($T_c \simeq 97$ K, open triangles), the second reference piece at the beginning of the second cycle ($T_c \simeq 87$ K, open circles) and the fourth reference piece before the last cycle ($T_c < 77$ K, full circles).

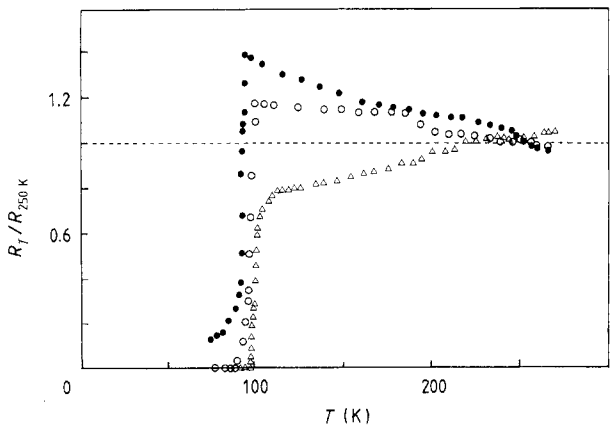


**Figure 2.** Resistance plotted against temperature: △, before the first thermal cycle; ○, before the second thermal cycle; (●), after evacuation at 623 K for 2 h.

A multi-function IF torsion pendulum system (MFIFA-I, made by the Institute of Solid State Physics, Academia Sinica) was used for the mechanical measurements. The 1 mm × 4 mm × 50 mm specimen was enclosed in a liquid-nitrogen Dewar with the torsion set-up and the three remaining reference pieces, to obtain a wide range of temperatures. At the heating stage, the temperature was increased in steps of 5 K from room temperature to 623 K and stable IF peaks $P_n$ were observed. Low-temperature IF measurements will not be discussed in this paper. We used a forced-oscillation mode in order to cover a wide frequency range. The maximum $Q^{-1}$ was found to be about $0.05 \pm 5 \times 10^{-4}$ and the accuracy of $Q^{-1}$ is about 1%. Temperature fluctuation does not exceed 0.2 K.

## 3. Results

Figures 3(*a*), 4(*a*), 5 and 6 show curves of $Q^{-1}$ against $T$ and of $G$ against $T$ for the first, second, third and fourth cycles (at the heating stage), respectively. In each figure, five curves correspond to five frequencies (in hertz) used in our experiment, as indicated in table 2.

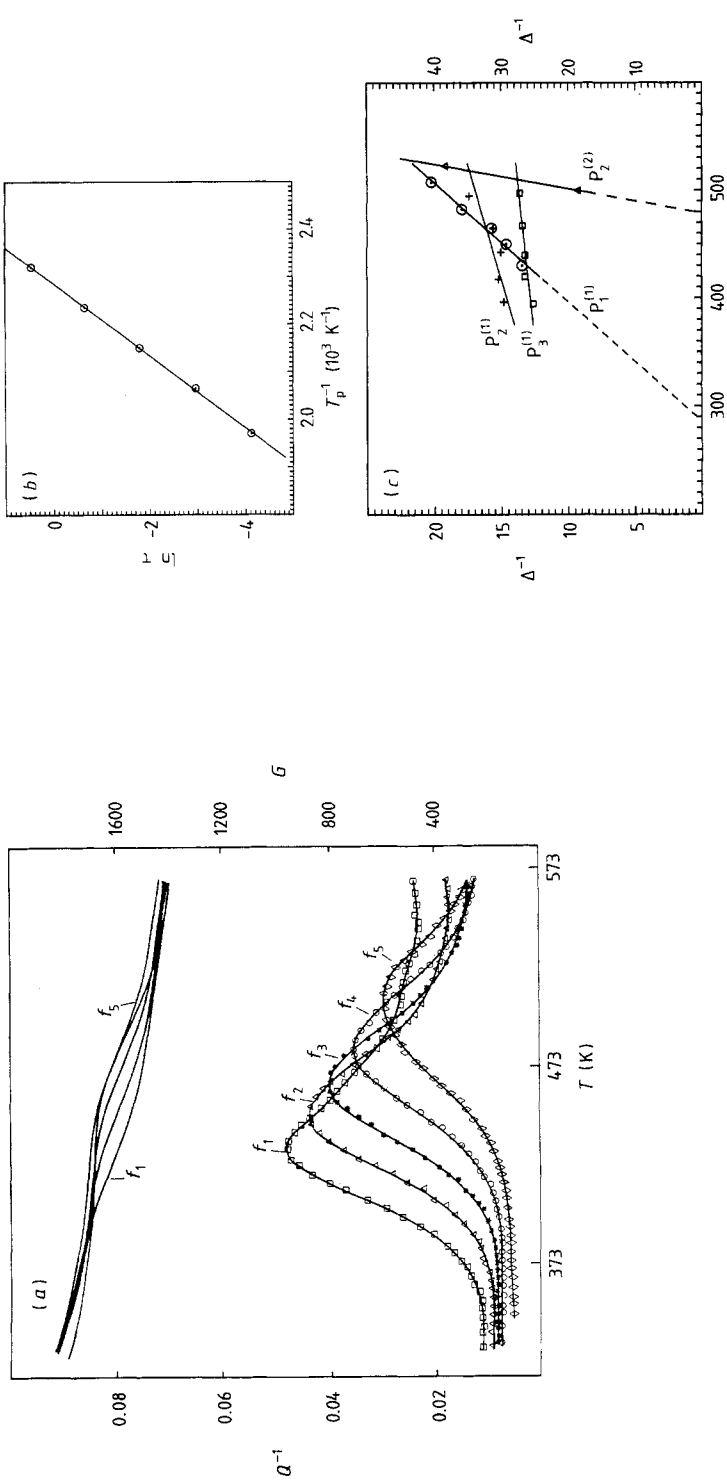


**Figure 3.** (*a*) IF and relative shear modulus plotted against temperature during the first thermal cycle for five frequencies (see table 2); (*b*) ln $\tau$ plotted against $1/T_p$ for the curves in (*a*); (*c*) Reciprocal relaxation strength $\Delta^{-1}$ plotted against temperature $T$ for curves from figures 3(*a*), 4(*a*) and 6; $P_n^{(m)}$ indicates the peak where $n$ is the peak number and $m$ the cycle number. The scale on the left-hand side should be used for lines $P_1^{(1)}$, $P_2^{(1)}$ and $P_3^{(1)}$ while the scale on the right-hand side should be used for line $P_2^{(2)}$.

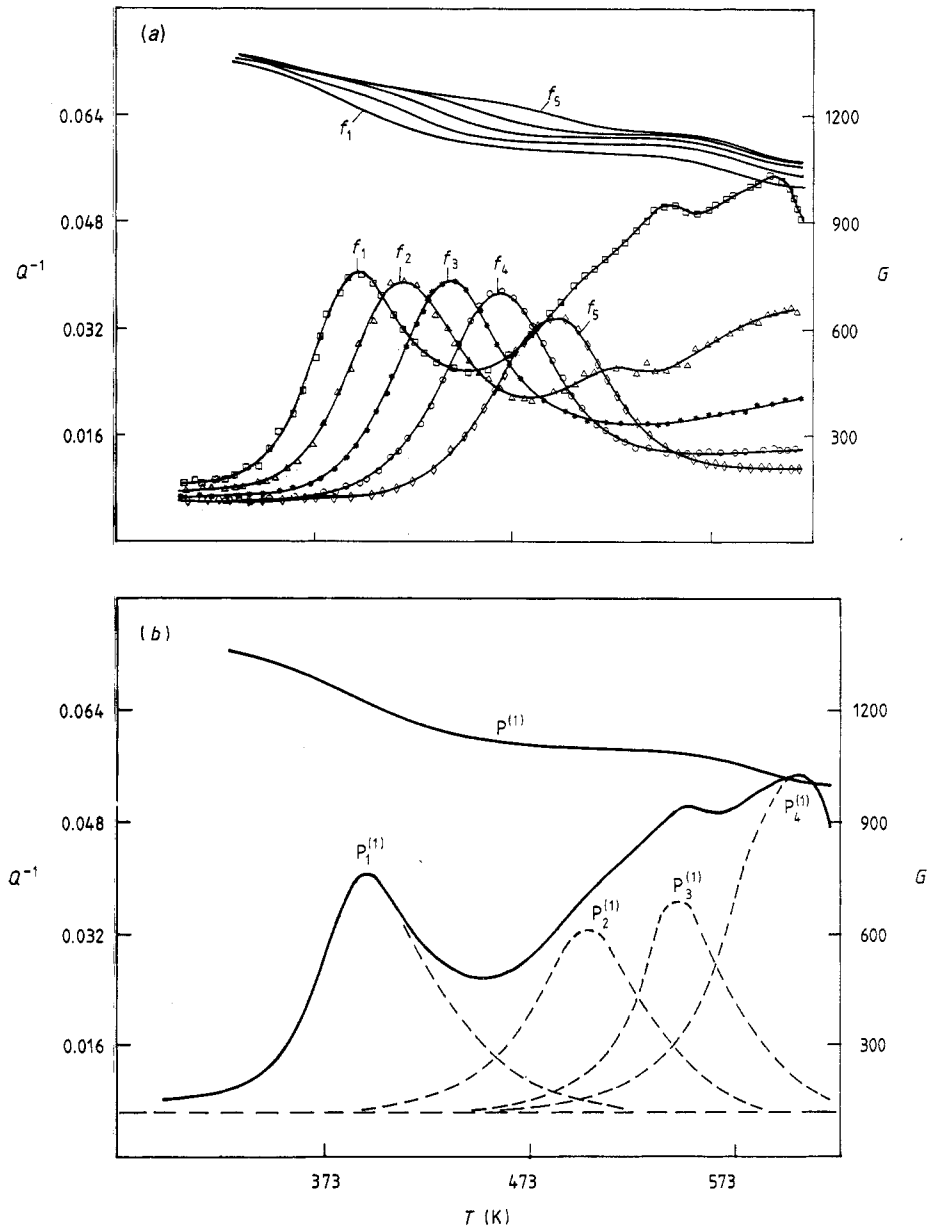


**Figure 4.** (*a*) IF and relative shear modulus plotted against temperature during the second thermal cycle for five frequencies (see table 2); (*b*) The decomposition of the $Q^{-1}$–$T$ curve for $f_1$ in (*a*); $P_n^{(m)}$ indicates the peak where $n$ is the peak number and $m$ the cycle number. Note that the decomposition is in general not unique.

From these results, the peak temperature $T_p$, the relaxation strength $\Delta$ ($\Delta = 2Q_p^{-1}$, where p indicates peak) and the relaxation time $\tau$ are determined. The slope of the Arrhenius graph of ln $\tau$ against $T_p^{-1}$ (figure 3(*b*)) gives the activation energy, and the $T$ axis intercept of the $\Delta^{-1}$ against $T$ graph provides the critical self-induced ordering temperature $T_c'$. The results are summarised in table 3.

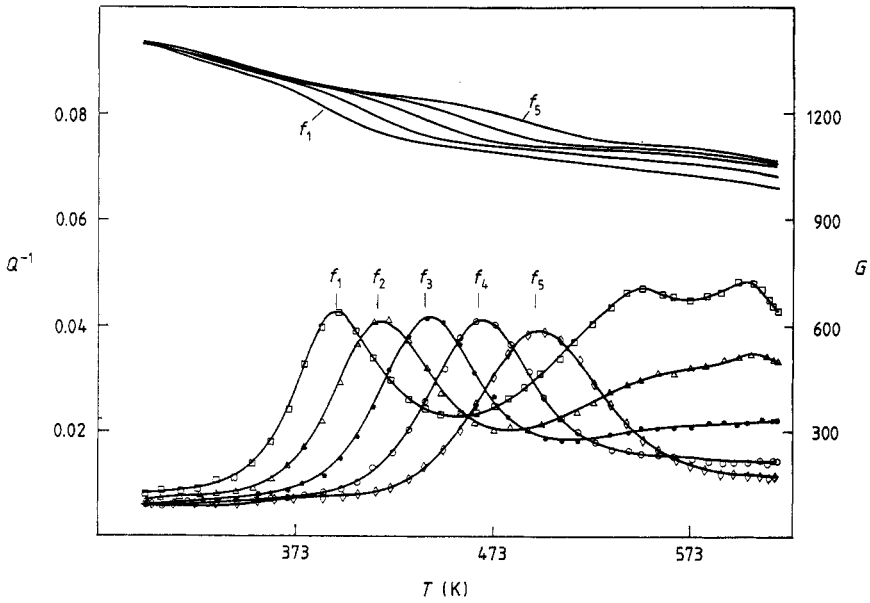


**Figure 5.** IF and relative shear modulus plotted against temperature during the third thermal cycle for five frequencies (see table 2).

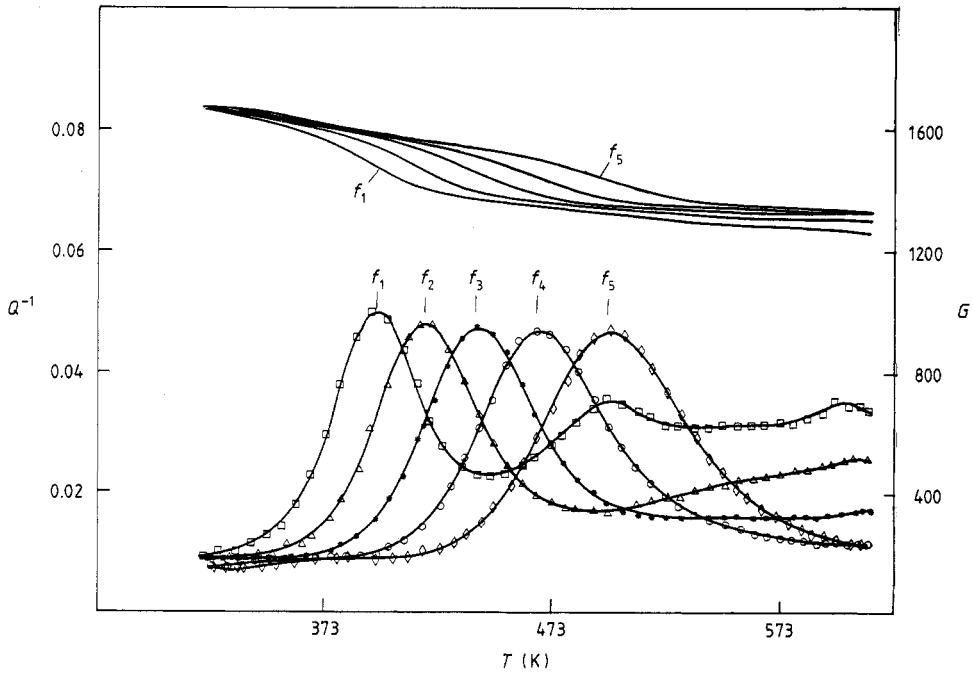


**Figure 6.** IF and relative shear modulus plotted against temperature during the fourth thermal cycle for five frequencies (see table 2).

**Table 2.** Different frequencies for various thermal cycles.

| | Frequency (Hz) | | | | |
|---|---|---|---|---|---|
| Cycle | $f_1$ | $f_2$ | $f_3$ | $f_4$ | $f_5$ |
| First | 0.100 | 0.316 | 1.00 | 3.16 | 10.0 |
| Second, third and fourth | 0.0100 | 0.0473 | 0.224 | 1.057 | 5.00 |

The temperature dependence of $Q^{-1}$ and $G$ during the first heating stage are relatively simple (figure 3($a$)), and such a dependence corresponds to metal-type $R$–$T$ behaviour (figure 2). There is an IF peak corresponding to each of the five oscillation frequencies, and the peak height decreases with increasing frequency (i.e. increasing peak temperature). Figures 3($b$) and 3($c$) show graphs of $\ln \tau$ against $T_p^{-1}$ and of $\Delta^{-1}$ against $T$, respectively. The self-induced ordering temperature $T_c' = 280$ K is indicated in figure 3($c$) (curve $P_1^{(1)}$). The behaviours of the $Q^{-1}$–$T$ and $G$–$T$ curves during the second heating stage are more complicated (figure 4($a$)); these curves correspond to semiconductor-type $R$–$T$ behaviour (figure 2). The differences between peaks at different frequencies are significantly reduced so that the $\Delta^{-1}$–$T$ curve (figure 3($c$), curve $P_2^{(1)}$) is flattened and has a negative intercept at the $T$ axis. Hence, no 'self-induced' ordering exists, which implies that the ordering of oxygen vacant sites represented by this peak has been destroyed. However, the relaxation strength determined by the $Q^{-1}$ peak height is noted to increase at the higher temperature (above 473 K), which indicates the enhancement of a new relaxation process, and figure 4($b$) shows the decomposition of the $Q^{-1}$–$T$ curve (for $f_1$) into four peaks $P_1^{(1)}$, $P_2^{(1)}$, $P_3^{(1)}$ and $P_4^{(1)}$. The first peak $P_1^{(1)}$ is the most pronounced and the variation in the peak temperature with frequency gives the activation energy $H$. The temperature dependence of the second peak $P_2^{(1)}$ is associated with a higher activation energy than is the first peak: $1.5 \pm 0.1$ eV. The relaxation strength of peak $P_2^{(1)}$ also gives another self-induced ordering temperature $T_c'$ of 480 K (figure 3($c$), curve $P_2^{(2)}$, noting its different coordinate scaling), which shows that $P_2^{(1)}$ is associated with the migration of ordered oxygen vacant sites. The third heating stage provides similar information to that provided by the second stage (figure 5).

The results of $Q^{-1}$–$T$ and $G$–$T$ relations for the fourth increasing-temperature process are shown in figure 6. Peak $P_2$ can now be distinguished (especially in the $f_1$ curve) because of the reduction in peak $P_3$. From a comparison of the $f_1$ and $f_2$ curves, it can be seen that the $P_2$ intensity decreases quickly with increase in frequency (i.e. peak-temperature increase) because $P_2$ is flattened significantly in the $f_2$ curve. Therefore, we consider that $P_2$ is still associated with the migration of ordered oxygen vacancies. This means that the corresponding $\Delta^{-1}$–$T$ curve for $P_2$ gives a positive $T_c'$.

## 4. Discussion

In our experiments, when a specimen undergoes heating at a low oxygen pressure the oxygen deficiency $\delta$ is gradually increased (Jorgensen *et al* 1987). Although no direct measurement of $\delta$ was carried out for the reference pieces, the relaxation strengths of the first ($P_1$) and the second ($P_2$) relaxation processes do increase as the thermocycles proceed (table 3). On the contrary, $\tau_0$ for the relaxation process was found to be about

**Table 3.** Summary of results.

| Sample condition when $Q^{-1}$ and $G$ are measured | $T_c$ ($R = 0$) (K) | Onset temperature $T_c^{(m)}$ (K) | Type of $R$–$T$ curve | Activation energy $H_1$ of first relaxation (eV) | $T_c'$ of first relaxation (K) | Strength $\Delta_1$ of first relaxation | Strength $\Delta_2$ of second relaxation |
|---|---|---|---|---|---|---|---|
| (i) Sample B: immediately after annealing in an oxygen atmosphere at about 1 atm pressure | 97 | 120 | Metallic | 1.12 | 280 K | $\simeq 0.060$ | $\simeq 0.04$ |
| (ii) Sample B: after first thermal cycle; pressure of air atmosphere, 60 Torr | 89 | 105 | Semiconductor | 1.06 | — | $\simeq 0.070$ | $\simeq 0.05$ |
| (iii) Sample B: after second thermal cycle; pressure of air atmosphere, 60 Torr | — | — | — | $1.03_5$ | — | $\simeq 0.075$ | $\simeq 0.05$ |
| (iv) Sample B: after third thermal cycle; pressure of atmosphere, $10^{-2}$ Torr | 77 | 95 | Semiconductor | $1.01_5$ | — | $\simeq 0.080$ | $\simeq 0.06$ |

$10^{-13}$–$10^{-14}$ s for all peaks; this is a typical value of the preliminary relaxation time for a point defect (Nowick and Berry 1972). Hence, the relaxation processes associated with $P_1$ and $P_2$ in this experiment pertain to oxygen vacant sites. These processes become more marked with decrease in oxygen stoichiometry. It is well established that $T_c'$ represents the critical temperature for a 'self-induced' ordering. The free energy of the system is lowest when the vacant sites are completely ordered. For peak $P_1^{(1)}$, $T_c' = 280$ K and $kT_c'$ (= 0.023 eV) represents the free-energy decrease due to an ordering process of one vacancy. For peaks $P_2^{(2)}$ and $P_2^{(3)}$, meaningful (i.e. positive) values of $T_c'$ were also determined. These show that oxygen vacancies are partly ordered in the approximate temperature range 400–500 K. In the meanwhile, although the specimen is still superconducting (with lower $T_c$ values of 89 K and less than 77 K, respectively for the second and fourth cycles), peak $P_1$ does not give any meaningful $T_c'$. Hence, the oxygen vacancies associated with $P_1$ do not need to be ordered for superconductivity to occur. Ordering associated with $P_1$, however, increases the superconducting efficiency.

The experiment suggests that the first relaxation process ($P_1$) can be associated with both ordered oxygen vacancies (if $\delta$ is small) and disordered oxygen vacancies (if $\delta$ increases), and the second relaxation process ($P_2$) is always associated with ordered vacancies, as long as the specimen conserves the orthorhombic structure and high-$T_c$ superconducting properties. Furthermore, it can be concluded that the metal-type $R$–$T$ behaviour corresponds to ordered oxygen vacant sites, and the semiconductor-type behaviour corresponds to disordered oxygen vacant sites associated with peak $P_1$ and ordered oxygen vacancies associated with peak $P_2$. It is consistent with the previous assumption of a metal–semiconductor transition in such ceramic superconductors (Derouane *et al* 1987).

To ascertain probable migration processes associated with the IF peaks $P_1$ and $P_2$, we consider the questions in § 1 in sequence. X-ray and neutron diffraction techniques provide measurement of the oxygen deficiency rate of different positions in high-$T_c$ orthorhombic $YBa_2Cu_3O_{7-\delta}$ (table 4), and such a result reflects possibilities of oxygen vacancy generation at positions 1, 2, 3, 4 and 5. Here, V($x$) denotes oxygen vacancy site at position $x$ and O($x$) the oxygen site at $x$. Table 4 indicates that the oxygen deficiency

**Table 4.** The oxygen deficiency rate at different positions in high-$T_c$ orthorhombic $YBa_2Cu_3O_{7-\delta}$ (determined by neutron diffraction techniques).

| | Oxygen deficiency rate (%) for the following vacancies | | | | |
|---|---|---|---|---|---|
| Reference | V(1) | V(2) | V(3) | V(4) | V(5) |
| Strobel *et al* (1987) | 7 | 3 | 1 | 3 | 100 |
| Jorgensen *et al* (1987) | 35 | 0 | 0 | 0 | 94 |
| David *et al* (1987) | 0 | 7.5 | 0 | 0 | — |

rate is sensitive to sample preparation and heat treatment. Consequently, the possibility that O(1), O(2) and sometimes O(4) migrate away is large enough to produce an anelastic process with $\Delta$ of the order of $10^{-2}$ (Nowick and Berry 1972).

According to the thermodynamic selection rule of point-defect relaxation for anelasticity, relaxation processes may occur for those point defects whose symmetry is lower

than that of the crystal. In the $YBa_2Cu_3O_{7-\delta}$ crystal, not only position 1 but also positions 2, 3 and 4 do have lower symmetries than that of the crystal because they deviate from the plane of copper or barium ion. Hence, an anelastic IF peak may be associated with one of the migration processes between the following pairs:

$$\begin{array}{lcl} \mathrm{V(1)} \leftrightarrow \mathrm{O(4)} & \mathrm{O(2)} & \mathrm{V(2)} \leftrightarrow \mathrm{O(3)} \\ & \swarrow \quad \nearrow & \\ & \mathrm{V(4)} & \\ & \nwarrow \quad \searrow & \\ \mathrm{O(1)} \leftrightarrow \mathrm{V(5)} & \mathrm{O(3)} & \mathrm{V(3)} \leftrightarrow \mathrm{O(2)}. \end{array}$$

Applying an oscillating stress to the polycrystalline specimen, some relaxation processes are more likely to occur than others. A compressing stress along the $z$ axis tends to affect O(4) migration in order to lower the elastic energy. O(4) on layer 3 or 5 most probably migrates to V(1) on layer 4 rather than to V(2) because the Cu(2)–O(4) bond is much longer than the Cu(1)–O(1) bond (Miceli *et al* 1988). If the compressing stress is changed to a tensile stress, the opposite migration process occurs. Hence, an anelastic relaxation process would be observed if an oscillating stress is applied. Similarly, an oscillating stress along the O$x$ (or O$y$) direction will benefit migrations between O(1) ↔ V(4) and O(3) ↔ V(2) (or O(2) ↔ V(3) and O(2) ↔ V(4)) and anelastic relaxation processes would be observed. The possibility of filling V(5) is ignored because this would mean a phase transition rather than a relaxation which we are considering in this work. The above-mentioned migration processes can thus be divided into two types as follows: type I is

$$(\mathrm{O}x \text{ or } \mathrm{O}y) \begin{cases} \mathrm{V(2)} \leftrightarrow \mathrm{O(3)} \\ \mathrm{V(3)} \leftrightarrow \mathrm{O(2)} \end{cases} \qquad \text{in the same layer}$$

and type II is

$$\begin{array}{ll} (\mathrm{O}z) & \mathrm{V(1)} \leftrightarrow \mathrm{O(4)} \\ (\mathrm{O}x) & \mathrm{V(4)} \leftrightarrow \mathrm{O(1)} \end{array} \qquad \text{between different layers.}$$

When applying a torsion shear stress to polycrystalline Y–Ba–Cu–O ceramics, a longitudinal oscillating stress along all the O$x$, O$y$, O$z$ directions occurs for grains (Nowick and Berry 1972). However, for every grain, it is expected that the stress along one direction will be predominant so that only one type of relaxation process is most likely to occur. The type II relaxation process concerns the migration of vacant sites between two layers and there is only one possibility for it to happen. Hence, the type II relaxation process is associated with an ordered oxygen deficiency as long as the orthorhombic structure is maintained. Since the orthorhombicity of the structure is very sensitive to the V(1)-to-O(1) ratio, the configuration of oxygen vacancies, which has been disturbed by the oscillating stress, tends to recover after unloading. This means that the oxygen vacancy sites recover their original states. However, the type I relaxation process concerns migration between not only ordered oxygen vacancies but also disordered oxygen vacancies. When $\delta$ is very small (or the specimen is undergoing annealing), only V(2) exists on layer 2 or layer 6. Then the migration process is associated with only ordered oxygen vacancies. When $\delta$ increases (or the specimen is undergoing thermal cycles), the ordering configuration of oxygen vacancies is disturbed because not only V(2) but also V(3) appears and two different relaxation processes V(2) ↔ O(3) and V(3) ↔ O(2) may occur simultaneously. Note that V(2) and O(3) (or O(2) and V(3))

may exchange after unloading since the difference between positions 2 and 3 is relatively small, and the V(2)-to-O(3) and V(3)-to-O(3) ratios are not sensitive to the phase transition in the crystal. Since the orthorhombicity of structure is not sensitive to the V(2)-to-O(2) and V(3)-to-O(3) ratios, then V(2) and O(3) (or V(3) and O(2)) may exchange after unloading.

On the basis of the above discussion, we suggest that the IF peak $P_1$ is related to oxygen vacancy migration on layer 2 or layer 6, i.e. V(2) $\leftrightarrow$ O(3) and/or V(3) $\leftrightarrow$ O(2), and the IF peak $P_2$ to oxygen vacancy migration between layer 3 or 5 and layer 4. Because the energy barrier for migration between layers is larger than that on the same layer, the activation energy for $P_2$ is larger than that for $P_1$.

As thermal cycles proceed, the oxygen deficiency $\delta$ increases and the Cu(1)–O(4) bond length as well as the lattice parameter ratio $(b - a)/a$ decreases. These results lead to a decrease in energy barrier for both $P_1$ and $P_2$ as listed in table 3.

In summary, the IF study of the Y–Ba–Cu–O ceramics reveals that the oxygen vacancy relaxation processes occur on the Cu(2)–O(4) planes first, which is followed by a relaxation process along the Cu–O chain when the temperature increases. From our study, we believe that the occurrence of a relatively high $T_c$ ($T_c^{R=0} \geqslant 90$ K) and metallic-type behaviour are associated with ordered oxygen deficiency in both the Cu(1)–O(2) chain and the Cu(2)–O(4) plane. When the oxygen deficiency in the Cu(2)–O(4) plane is disordered, the superconductive transition still occurs but the value of $T_c^{R=0}$ decreases.

## References


Chen T G, Zhang J H, Huang J and Chen Y 1987 *Proc. Workshop High $T_c$ Superconductivity* (Peking: Chinese Academic Press)

David W I F, Harrison W T A, Gunn J M F, Moze O, Soper A K, Day P, Jorgensen J D, Beno M A, Capone D W, Hinks D G, Schuller I K, Soderholm L, Segre C U, Zhang K and Grace J D 1987 *Nature* **327** 310–2

Derouane E G, Gabelica Z, Brédas J L, André, Lambin P, Lucas A A and Vigneron J P 1987 *Solid State Commun.* **64** 1061

Jorgensen J D, Beno M A, Hinks D G, Soderholm L, Volin K J, Hitterman R L, Grace J D, Schuller I K, Segtr C U, Zhang K and Kleefisch M S 1987 *Phys. Rev.* B **36** 3608

Lin G M, Huang Q Z, Zhang J X, Siu G G and Stokes M J 1988 *Solid State Commun.* **68** 639–41

Luo Y J, Zhang J X, Lin G M, Huang K Y, Huang Q Z, Du Z L and Xiao H Q 1987 *Proc. Beijing Int. Workshop High Temperature Superconductivity (Supplement)* (Beijing: Chinese Academic Press) pp 128–31

Miceli P F, Jarascon J M, Greene L H, Barboux P, Rotella F J and Jorgensen J D 1988 *Phys. Rev.* B **37** 5932–5

Nowick A S and Berry B S 1972 *Anelastic Relaxation in Crystalline Solids* (New York: Academic)

Strobel P, Capponi J J, Marezio M and Monod P 1987 *Solid State Commun.* **64** 513

Van Tendeloo G, Zandbergen H W, Okabe T and Amelinckx S 1987 *Solid State Commun.* **63** 969